Scanning Microscopy

Volume 1 | Number 4 Article 49

7-19-1987

Fictitious Calculi and Human Calculi with Foreign Nuclei

P.-T. Cheng
University of Toronto

K. P. H. Pritzker
University of Toronto

J. Richards
University of Toronto

D. Holmyard
University of Toronto

Scanning Microscopy, Vol. 1, No. 4, 1987 (Pages 2025-2032)
Scanning Microscopy International, Chicago (AMF O'Hare), IL 60666 USA

0891-7035/87$3.00+.00

FICTITIOUS CALCULI AND HUMAN CALCULI WITH FOREIGN NUCLEI

P.-T. Cheng*, K.P.H. Pritzker, J. Richards and D. Holmyard

Department of Pathology
Mount Sinai Hospital
University of Toronto
Toronto, Canada

(Received for publication April 09, 1987, and in revised form July 19, 1987)

Abstract

The correlative approach employing polarized light microscopy, x-ray powder diffraction, scanning electron microscopy, transmission electron microscopy, selected area electron diffraction and energy dispersive x-ray microanalysis proves to be very useful in identifying fictitious calculi and genuine human calculi with foreign body nuclei. The common artifacts as reported in the literature and observed also by us were minerals, vegetable and plant seeds, cereals, sand grains and sea shell fragments.

Two interesting cases involving foreign body nuclei have been reported: one urinary calculus containing a piece of plastic-coated titanium foil in the center; one nasal calculus with a nut as a nucleus. Another common cause for foreign body nucleation is iatrogenic: intrauterine devices, catheters, suture materials and even surgical staples have been reported in the literature to be potent nidi for calculus formation.

These cases remind us of the important fact that our body fluids are supersaturated with respect to calcium phosphates and occasionally to other compounds. Hydroxyapatite crystals are readily nucleated by foreign bodies. Whitlockite is involved if the fluid Mg/Ca ratio is in a suitable range, brushite if the fluid is acidic and struvite if there is urea-splitting infection. In urine and other fluids, calcium oxalate and uric acid crystals contribute to the calculus growth.

KEY WORDS: Fictitious calculi, nasal calculus, calculi with foreign nuclei, iatrogenic calculi, x-ray diffraction, scanning electron microscopy, x-ray microanalysis, transmission electron microscopy, selected area electron diffraction.

*Address for correspondence:
P.-T. Cheng, Department of Pathology, Mount Sinai Hospital, 600 University Avenue, Toronto, Canada, M5G 1X5. Phone no. (416) 586-4468

Introduction

Over the past 10 years, we have analyzed over 1000 human urinary and non-urinary calculi in our laboratory. As experienced by Herring (1962) and by Prien (1963), approximately 1% (9) of the specimens submitted for analysis turned out to be of non-human origin. The common artifacts as reported in the literature and observed also by us were alloys (2), minerals (2), vegetable and plant seeds (2), cereals, sand grains (2) and sea shell fragments (1). Also 3 genuine human calculi, 1 urinary and 2 non-urinary, had foreign body nuclei (cases 4-6). Prien (1963) also reported that a few such artificially induced calculi had been removed from the bladders of women at cystoscopy. Foreign body nuclei have also been found in salivary calculi (Wakeley, 1929).

Another common cause for foreign body nucleation of genuine calculi is iatrogenic. Suture materials (cotton, silk, chromic catgut, polypropylene, etc.), catheters (Kiryabwire and Shah, 1969) and even surgical staples have been shown to be potent nidi for calculus development (Straffon and Higgins, 1970; Healey and Warren, 1979; Norris et al., 1982; Brenner and Johnson, 1985). Urinary calculi nucleated by migrant intrauterine devices have also been reported (Saronwala et al., 1974; Neutz et al., 1978; Woods and Wise, 1980).

An area related to foreign body induced calculi is calculus development in the gut or in the urinary tract after oral intake of drugs and chemicals. Ethylene glycol poisoning is well known for the risk of developing calcium oxalate urinary calculi (Parry and Wallach, 1974; Godolphin et al., 1980). Carbonic anhydrase inhibitors such as acetazolamide and methazolamide may induce urinary calculi (Ellis, 1973). Long term use of antacids (calcium carbonate, sodium bicarbonate and magnesium trisilicate) have been associated with urolithiasis (Joekes et al., 1973; Isenberg, 1979; Farber and Rajfer, 1984).

Although fictitious calculi and foreign body induced calculi are of great interest both clinically and analytically, the literature on the analytical aspects of these materials is very scarce. Here we report our experience on the analysis of these calculi by correlative polarized light microscopy (PLM), x-ray powder diffraction (XRD), scanning electron microscopy (SEM), transmission electron microscopy (TEM), selected area electron diffraction (SAED) and energy dispersive x-ray microanalysis (EDX).

Materials and Methods

PLM and XRD were the routine methods employed in our laboratory to analyze urinary and non-urinary calculi submitted by urologists, nephrologists, surgeons and other clinicians. When the identification was not straight forward or when the specimen proved to be of particular interest, e.g., of non-human origin or having a foreign body nucleus, then SEM, TEM, SAED and EDX would also be employed. The methodology used was similar to that published before (Cheng et al., 1981; 1983; 1985; Cheng and Reid, 1985).

X-ray powder diffraction

One-half of each small calculus was gently powdered and transferred into 0.3 mm Lindermann capillary tubes. XRD patterns were obtained in a 114.6 mm Debye-Scherrer powder camera exposed to Ni-filtered CuKα radiation and compared with published results (Sutor and Scheidt, 1968). Large calculi were fractured and representative samples were removed from the fracture surfaces for XRD analysis.

Analytical scanning electron microscopy

Specimen powder removed from the Lindermann tube was then mounted on aluminum stubs and coated with either carbon or gold. The stubs were then examined in a Hitachi S-520 scanning electron microscope equipped with a Tracor Northern 2000 EDX system. For larger calculi, fracture surfaces were studied instead.

Analytical transmission electron microscopy

The other half of the specimen not used for XRD and SEM was fixed in 2% glutaraldehyde, then fixed in 1% cacodylate-buffered osmium tetroxide, dehydrated in graded alcohols and embedded in Spurr's resin. 0.5 μm sections were cut and stained with toluidine blue for PLM. 70 nm sections were also cut with a diamond knife, stained with 2% uranyl acetate and 1% lead citrate, or alternatively left unstained, and viewed with a Philips 430 high voltage scanning transmission electron microscope equipped with a Link AN 10000 EDX system. SAED patterns were obtained from crystal deposits at accelerating voltages of 60-300 kV.

Results and Discussion

Fictitious Calculi

As mentioned above, artifacts submitted to our laboratory as 'urinary calculi' included metal alloys, seeds and minerals. One example from each group is given below.

Case 1: Dental filler. A silvery metallic piece of approximately 4mm X 3mm X 3mm (Fig. 1) failed to register an XRD pattern because it was too bulky and could not be broken up easily. The EDX spectrum of the specimen indicated Hg, Sn and Ag as the major elemental components and Cu, Fe and Si as minor components (Fig. 2). This composition suggested that the specimen was a piece of dental amalgam alloy which was a union of Hg with a Ag-Sn alloy and usually contained a small amount of Cu (Skinner and Phillips, 1967).

Case 2: Bean. A 2mm bean-like substance with an orange coating and a whitish cortex gave an XRD pattern with no sharp peaks, consistent with that of an organic material. Histological sections showed a layer of plant cells forming the coating and the cortex filled with fibrous matrix (Fig. 3).

Case 3: Hydrozincite. Two light brown particles (3mm irregular) gave an XRD pattern hitherto unknown to us (Fig. 4). SEM showed the surface morphology not so different from that of a genuine urinary calculus (Fig. 5). However, the EDX spectrum indicated that Zn was the major metal present in the sample (Fig. 6). By comparing the observed d-spacings with those of several Zn-containing minerals as listed in Mineral Powder Diffraction File (Bayliss et al., 1980), the specimen was determined to be Hydrozincite, a mineral consisted of the basic zinc carbonate $Zn_5(CO_3)_2(OH)_6$ (Table 1).

Table 1. Observed d-spacings from the x-ray powder diffraction pattern of the mineral in Case 3 compared with those of hydrozincite.

Observed d-spacing nm	Relative Intensity	Hydrozincite d-spacing nm	Relative Intensity
0.685	VS	0.677	100
0.527	VW	0.537	10
0.403	VW		
0.368	VW	0.366	40
0.316	M	0.314	50
		0.300	10
		0.292	20
0.287	W	0.285	30
		0.274	10
0.271	VS	0.272	60
		0.269	20
0.260	M	0.258	10
0.247	S	0.248	70
0.233	W	0.234	10
		0.230	20

VS = very strong; S = strong; M = medium; W = weak; VW = very weak.

Genuine Calculi with Foreign Body Nuclei

Two very interesting cases are presented below; one urinary and one non-urinary.

Case 4: Plastic-coated titanium foil as nucleus. A flat whitish bladder calculus (1.5cm X 1.5cm) was removed from a young boy who had a neurogenic bladder and a previous bladder operation. The calculus split easily into two halves longitudinally, revealing in the center a piece of plastic-coated metal foil (4mm X 5mm) with a cellulose film on one side (Fig. 7). XRD patterns indicated that the mineral components of the calculus were struvite [$MgNH_4PO_4 \cdot 6H_2O$] and hydroxyapatite [$Ca_{10}(PO_4)_6(OH)_2$], consistent with those of a urinary calculus due to urea-splitting infection (Fig. 8). SEM showed large and small crystals attached to the cellulose film (Fig. 9) and EDX indicated titanium to be the metal of the foil (Fig. 10). Also observed were typical apatite crystal deposits at the foil-mineral interface (Fig. 11), and large struvite crystals, with characteristic 'Y' cracks on some faces (Kim, 1982), closer to the calculus surface (Fig. 12).

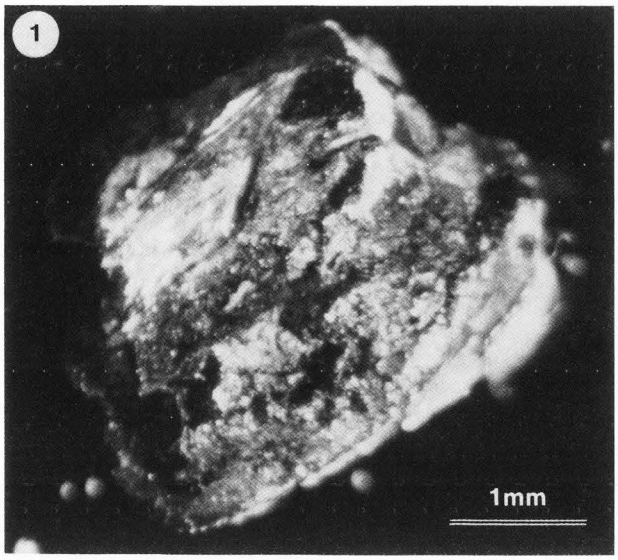

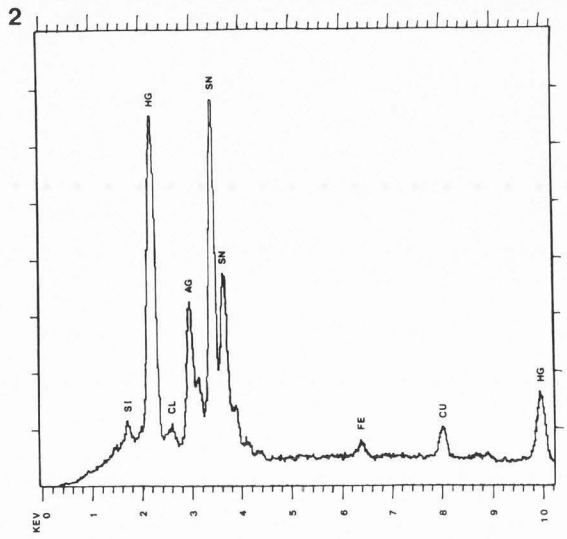

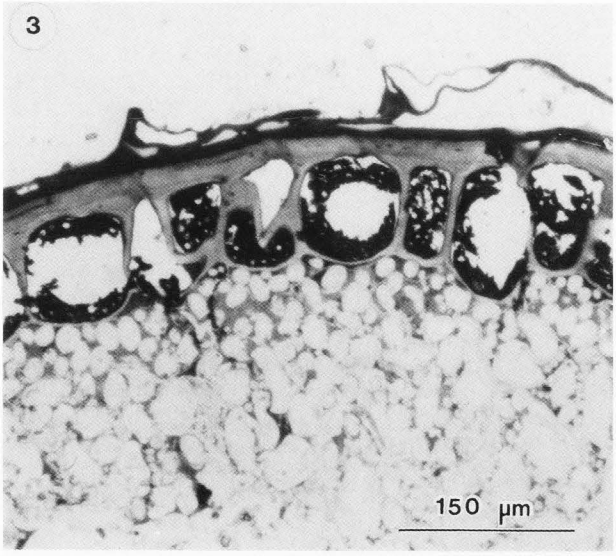

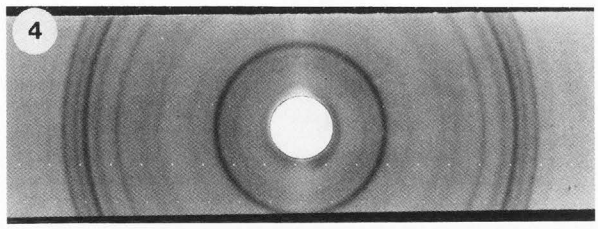

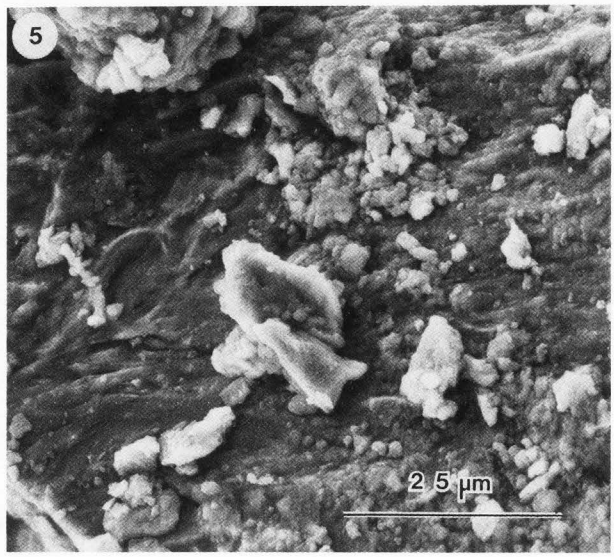

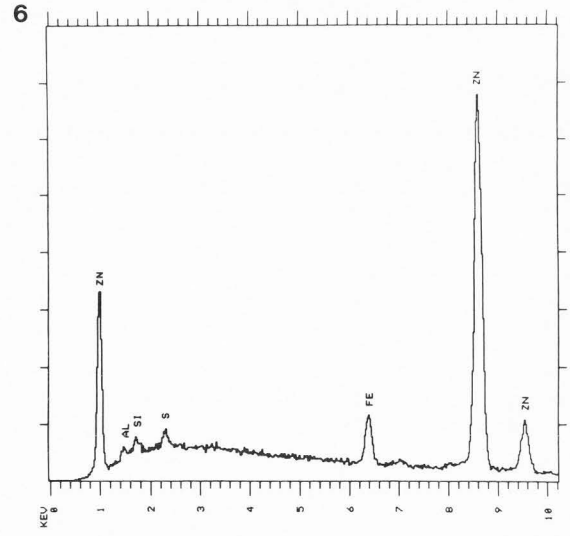

Fig. 1. Photomicrograph of the silvery metallic piece (Case 1).
Fig. 2. EDX spectrum of the metallic piece (Case 1).
Fig. 3. Histological section of a part of the bean (Case 2).
Fig. 4. XRD pattern of the mineral particles (Case 3).
Fig. 5. SEM view of the surface of a mineral particle (Case 3).
Fig. 6. EDX spectrum of the mineral particle (Case 3).

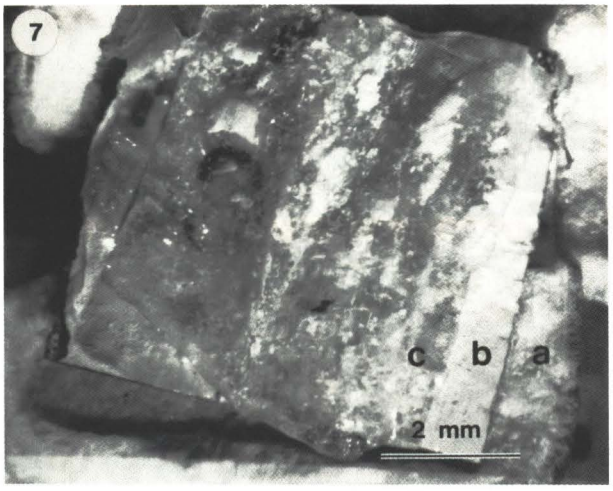

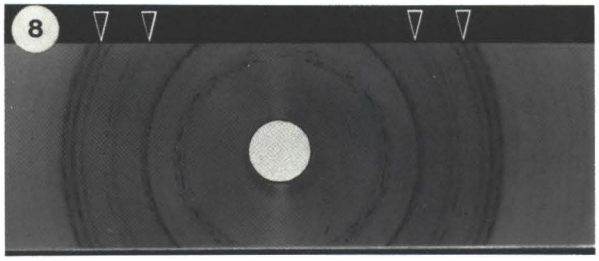

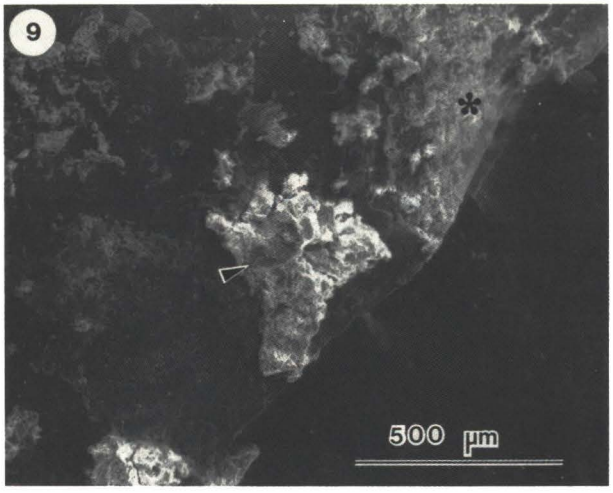

Fig. 7. Photomicrograph of one half of the bladder calculus (a) (Case 4) showing the presence of a piece of plastic-coated metal foil (b) with a cellulose film (c) attached to it.
Fig. 8. XRD pattern of the mineral components of the bladder calculus (Case 4) indicating the presence of struvite and apatite (arrow heads) crystals. Observed d-spacings in nm: 0.59 (S), 0.56 (S), 0.54 (S), 0.46 (VW), 0.425 (VS), 0.414 (S), 0.345 (M), 0.329 (MS), 0.292 (S), 0.28 (VS, diffuse), 0.268 (VS); VS = very strong, S = strong, MS = medium strong, M = medium, VW = very weak.
Fig. 9. SEM view of the cellulose film showing large (arrow head) and small (*) crystals (case 4).

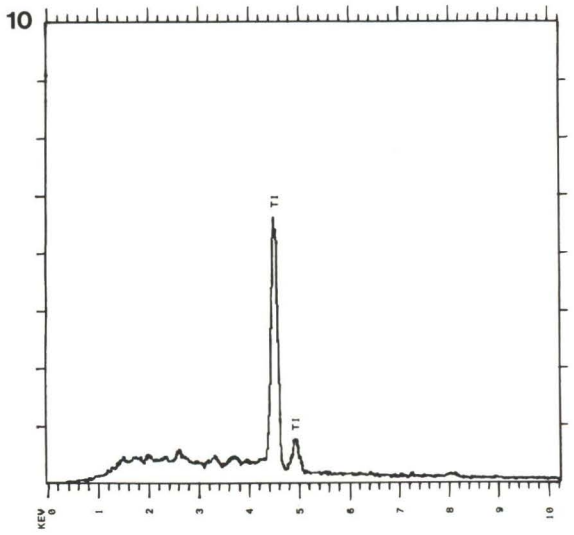

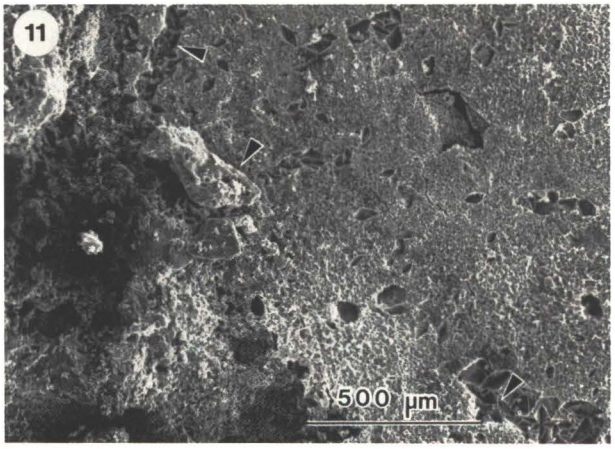

Fig. 10. EDX spectrum of the metal foil (Case 4).
Fig. 11. SEM view of the center of the bladder calculus (Case 4) showing the imprint of the foil at the foil-mineral interface, with the edge positions indicated by arrow heads.
Fig. 12. SEM view of the bladder calculus (Case 4) showing the presence of struvite crystals close to the calculus surface.

Case 5: Nut as nucleus. A whitish calculus with a diameter of approximately 1cm removed from the left nasal cavity of a young woman yielded a nut-like object in the center. XRD patterns indicated that hydroxyapatite was the mineral phase in the outer shell of the calculus (Fig. 13a). In the center of the 'nut' there was a pit which gave a different XRD pattern indicating the presence of calcium stearate crystals instead (Fig. 13b). As shown in Table 2, the observed d-spacings compared well with those of calcium stearate crystals (Sargent-Welch). The SEM view of the mineral-nucleus interface (Fig. 14) showed the usual submicronic apatite particles in close contact with the large plant cells of the nut shell. Lumps protruding from the plant cell surfaces were observed; apparently they could be scraped off easily from the cell surface (Fig. 15). This observation was supported by the TEM results which showed very thick cell walls for the plant cells and discrete electron dense inclusion bodies in the center of the cell as well as near the cell surface (Fig. 16). EDX spectra obtained from the electron dense bodies showed major Ca and P peaks and a minor Mg peak indicating that the plant cells were calcified, probably inside the nasal cavity (Fig. 17). However, the mineral involved was not identified since the SAED pattern did not match any of the known calcium phosphates. (Fig. 18).

Table 2. Observed d-spacings of the x-ray powder diffraction pattern of the pit of the nut in Case 5 compared with those of calcium stearate crystals.

Observed d-spacing nm	Relative Intensity	Calcium stearate d-spacing nm	Relative Intensity
1.592	VS	1.589	VS
1.181	VW	1.203	M
0.948	M	0.969	M
		0.805	VW
		0.700	VW
0.592	W	0.581	M
0.437	VS	0.438	VS
0.409	S	0.403	S
0.338	M	0.337	S
0.288	W	0.291	W
		0.283	VW
0.258	W		

VS = very strong; S = strong; M = medium; W = weak; VW = very weak.

Calculi Induced by Oral Intake of Drugs and Chemicals

We have not analyzed any urinary calculi in this category. Instead a non-urinary case is given below.

Case 6: Concretion in stomach. A white solid mass removed at autopsy from the stomach of a baby boy gave an XRD pattern identical to that of brushite [$CaHPO_4\ 2H_2O$] (Fig. 19). SEM showed large flat crystals with well developed faces up to 200 µm in length (Fig. 20); EDX spectra of same indicated Ca and P as major components (Fig. 21). The crystal morphology and elemental composition were in agreement with those of brushite; the formation of which was also favored by the acidic environment in the stomach. SEM also showed other particles without crystal faces (Fig. 20) and EDX of which showed major S peak in addition to Ca, Na, K and P (Fig. 22). These amorphous materials probably contained sodium polystyrene sulfonate, a cation exchange resin, which was administered orally to the boy as a treatment for hyperkalemia. Whether this resin promoted brushite crystal formation remained unknown.

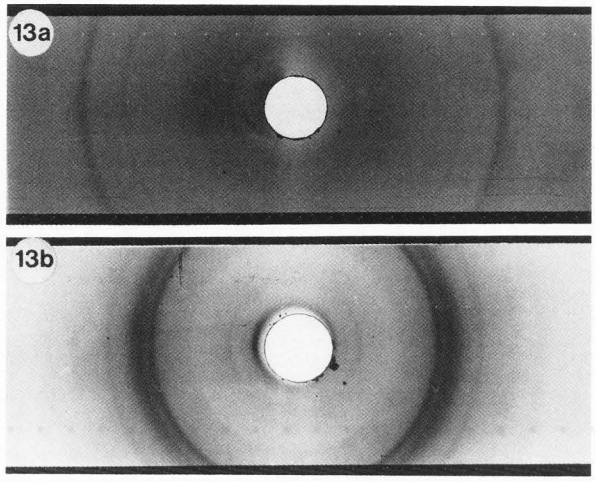

Fig. 13. a) XRD pattern of the outer shell of the nasal calculus (Case 5) indicating the presence of apatite crystals. Observed d-spacings in nm: 0.344 (medium), 0.28 (strong, diffuse). b) XRD pattern of the pit of the nut in the center of the nasal calculus indicating the presence of calcium stearate crystals.

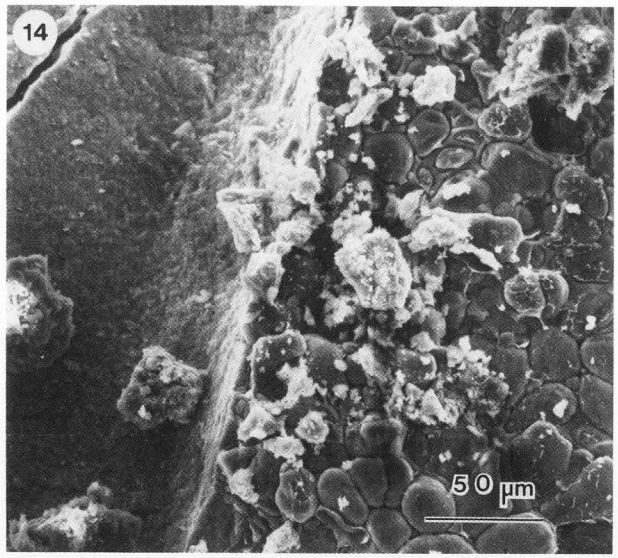

Fig. 14. SEM view of the nasal calculus (Case 5) showing the mineral-nut shell interface.

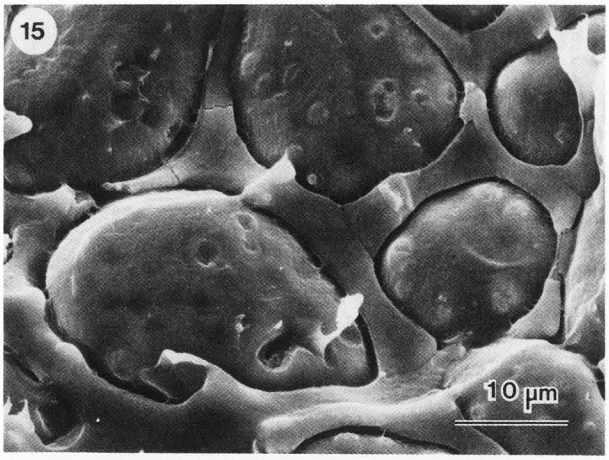

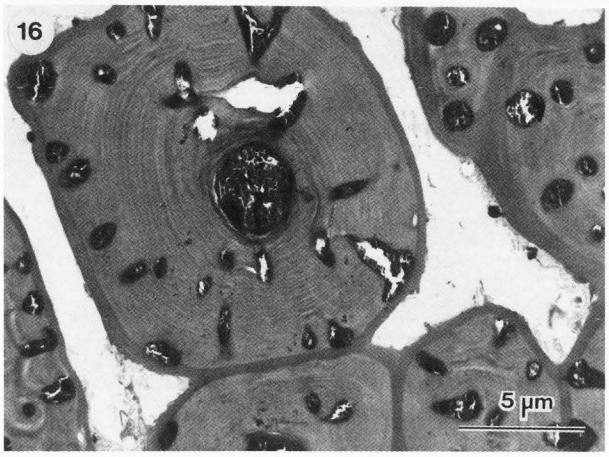

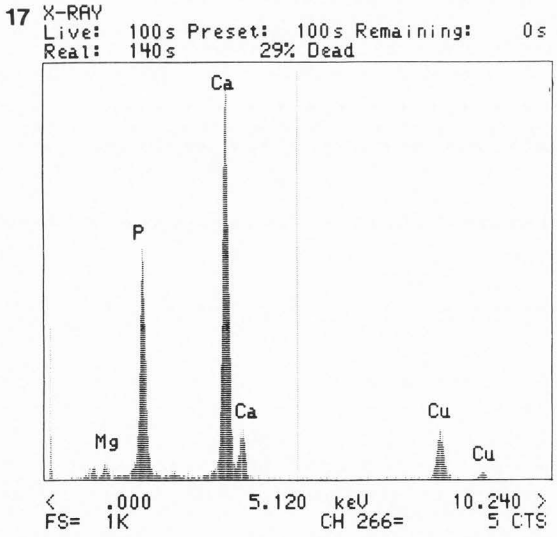

Fig. 15. SEM view of the surface of the nut shell showing lumps protruding from the surface (Case 5).
Fig. 16. TEM of a section of the nut shell showing plant cells with very thick cell walls and electron dense inclusion bodies (Case 5).
Fig. 17. EDX spectrum of the electron dense inclusion bodies as seen in Fig. 16.

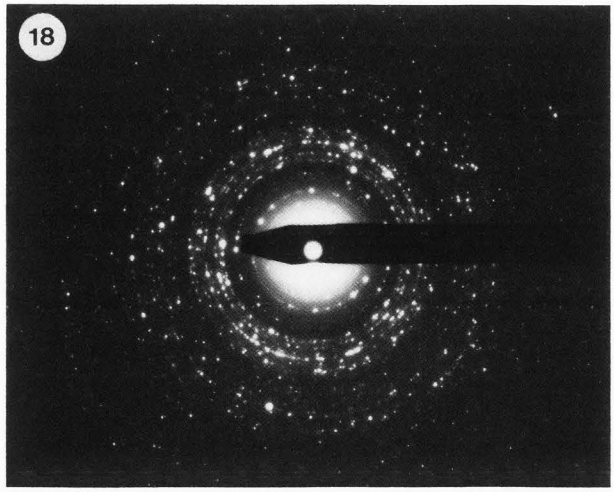

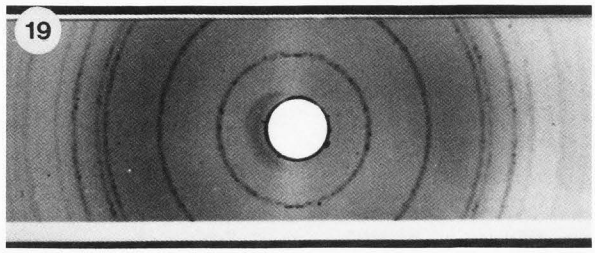

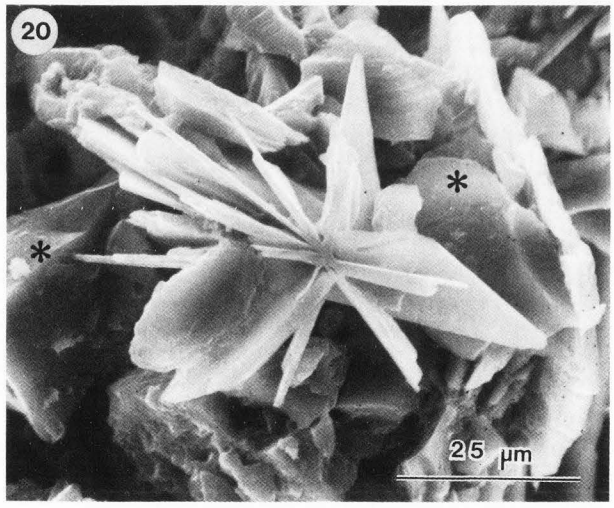

Fig. 18. SAED pattern of the electron dense inclusion bodies as seen in Fig. 16. Observed d-spacings in nm: 0.77 (W), 0.63 (M), 0.49 (S), 0.39 (M), 0.328 (S), 0.303 (S), 0.286 (W), 0.272 (S), 0.262 (M), 0.247 (M), 0.239 (M), 0.225 (W), 0.206 (W); S = strong, M = medium, W = weak.
Fig. 19. XRD pattern of the solid mass removed from the stomach of a baby boy (Case 6) indicating the presence of brushite crystals. Observed d-spacings in nm: 0.76 (VS), 0.425 (VS), 0.38 (VW), 0.304 (S), 0.293 (MS), 0.285 (VW), 0.261 (S); VS = very strong, S = strong, MS = medium strong, VW = very weak.
Fig. 20. SEM view of the stomach concretion (Case 6) showing large crystals with flat surfaces and other euhedral particles (*).

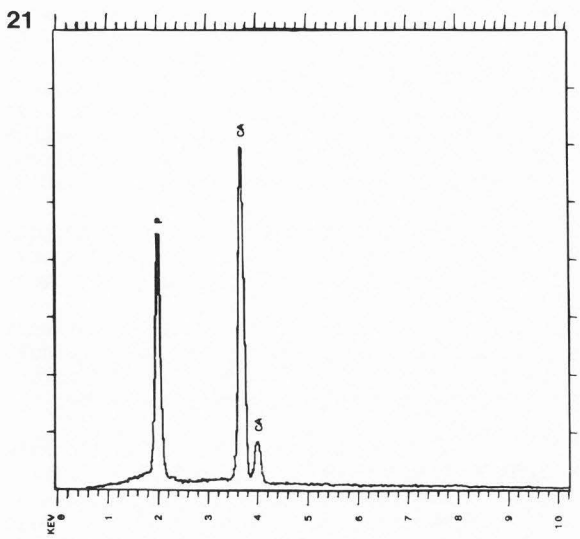

Fig. 21. EDX spectrum of the large crystals as seen in Fig. 20.

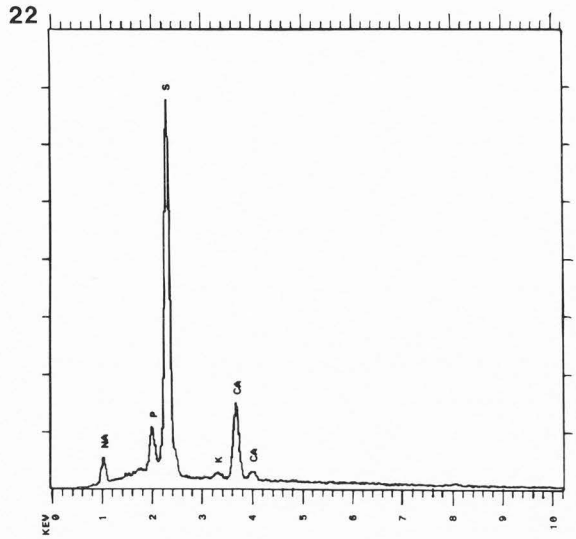

Fig. 22. EDX spectrum of the euhedral particles as seen in Fig. 20.

Conclusion

The correlative approach employing PLM, XRD, SEM, TEM, SAED and EDX proves to be very useful in calculus identification, including those with foreign body nuclei. Also this combined analytical technique permits us to identify fictitious calculi. Further improvement of this system could come from incorporation of other sophisticated analytical techniques including gas chromatography-mass spectrometry (Suvanich et al., 1984) and Fourier transform infrared spectrometry which should facilitate organic compound identification.

Cases 1-3 are examples of artifacts submitted as human calculi. The common artefacts including those reported here are alloys, minerals, vegetable and plant seeds, cereals, sand grains and sea shell fragments. Some of these artefacts are also found as foreign body nuclei in genuine calculi. Iatrogenic foreign body nuclei include migrant intrauterine devices, catheters, suture materials, surgical staples, wrapping materials, chemicals and drugs.

Cases 4-6 remind us of the important fact that our body fluids are supersaturated with respect to hydroxyapatite and sometimes other calcium phosphates. Foreign bodies, whatever their origin, composition and surface texture may be, are readily entombed in hydroxyapatite. Whitlockite is involved if the fluid Mg/Ca ratio is in a suitable range (≤1) (Cheng and Pritzker, 1983; Cheng, 1986), brushite if the fluid is acidic and struvite if there is urea-splitting infection. In urine and other fluids containing high levels of oxalate or urate, calcium oxalate and uric acid crystals contribute to the calculus growth.

Acknowledgment

We thank the Kidney Foundation of Canada for financial assistance.

References

Bayliss P, Berry LG, Mrose ME, Smith DK (eds.) (1980). Mineral Powder Diffraction File Search Manual. Joint Committee on Powder Diffraction Standards, Swarthmore, PA.

Brenner M, Johnson DE (1985). Ileal conduit calculi from stapler anastomosis: a long-term complication? Urology 26:537-540.

Cheng P (1986). Magnesium effects on de novo formation of calcium phosphate phases (abstract). J. Dent. Res. 65:801.

Cheng P-T, Pritzker KPH (1983). Solution Ca/P ratio affects calcium phosphate crystal phases. Calcif. Tissue Int. 35:596-601.

Cheng P-T, Pritzker KPH, Tausch J, Pittaway A, Millard J (1981). Analytical scanning electron microscopy and x-ray microdiffractometry of renal calculi using etched plastic sections. Scanning Electron Microsc. 1981; III:163-168.

Cheng P-T, Reid AD (1985). Low voltage scanning electron microscropy of uncoated kidney stones. Scanning Electron Microsc. 1985; IV:1551-1554.

Cheng P-T, Reid AD, Millard J, Pritzker KPH, Khanna R, Oreopoulos DG (1983). Ultrastructural studies of renal stones from patients on continuous ambulatory peritoneal dialysis. Scanning Electron Microsc. 1983; IV:1939-1946.

Cheng P-T, Reid AD, Pritzker KPH (1985). Ultrastructural studies of crystal-organic matrix relations in renal stones. Scanning Electron Microsc. 1985; I:201-207.

Ellis PP (1973). Urinary calculi with methazolamide therapy. Documenta Ophthalmologica 34: 137-142.

Farber JH, Rajfer J (1984). Silicate urolithiasis. J. Urol. 132:739-740.

Godolphin W, Meagher EP, Frohlich J, Sanders HD (1980). Letter. N. Engl. J. Med. 302:465-466.

Healey GB, Warren MM (1979). Stone formation on polypropylene suture. J. Urol. 121:836-837.

Herring L (1962). Observations on the analysis of ten thousand urinary calculi. J. Urol. 88: 545-562.

Isenberg JI (1979). Peptic ulcer: medical therapy. In: Cecil Textbook of Medicine, 15th. ed., Beeson PB, McDermott W. Wyngaarden JB (eds.) W. B. Saunders, Philadelphia, PA., part XVI, sect. 3, chapt. 405, pp. 1513-1516.

Joekes AM, Rose GA, Sutor J (1973). Multiple renal silica calculi. Br. Med. J. 1:146-147.

Kim KM (1982). The stones. Scanning Electron Microsc. 1982; IV:1635-1660.

Kiryabwire JWM, Shah RV (1969). Vesical stones due to a foreign body. East Afr. Med. J. 46:371-375.

Neutz E, Silber A, Merendino VJ (1978). Dalkon Shield perforation of the uterus and urinary bladder with calculus formation: Case report. Amer. J. Obst. Gynec. 130:848-849.

Norris MA, Toguri AG, Waguespack B (1982). Calcification on chromic suture. Urology 20:172-173.

Parry MF, Wallach R (1974). Ethylene glycol poisoning. Am. J. Med. 57:143-150.

Prien EL. (1963) Crystallographic analysis of urinary calculi: a 23-year survey study. J. Urol. 89:917-924.

Saronwala KC, Singh R, Dass H (1974). Lippes Loop perforation of the uterus and urinary bladder with stone formation. Obst. Gynec. 44:424-427.

Skinner EW, Phillips RW (1967). The Science of Dental Materials. W.B. Saunders, Philadelphia, PA., Chapt. 20, pp. 298-311.

Straffon RA, Higgins CC (1970). Urolithiasis. In: Urology, 3rd. ed., Campbell MF, Harrison JH (eds.), W. B. Saunders, Philadelphia, PA., vol. 1. chapt. 18, pp. 687-765.

Sutor DJ, Scheidt S (1968). Identification standards for human urinary calculus components using crystallographic methods. Brit. J. Urol. 40:22-28.

Suvanich S, Ambre J, Hobart E (1984). Pepper grains as artificial urinary calculi (letter). N. Engl. J. Med. 310:129.

Wakeley CPG (1929). The formation of salivary calculi and their treatment. Lancet 1:708-711.

Woods M, Wise Jr HM (1980). An unusual cause of cystolithiasis: A migrant intrauterine device. J. Urol. 124:720-721.

Discussion with Reviewers

N. Mandel: At the Veterans Administration Medical Center located at Milwaukee, WI, we established a similar stone analysis laboratory in 1983. Since that time we have analyzed over 12,000 stones by x-ray diffraction. The vast majority of these samples have been urinary tract calculi. We received approximately 1.2% non-human (artificial) stones. However, we have only received five genuine calculi with a foreign body nidus. Four were iatrogenical in origin, while the last was an automotive fuse. What accounts for the high incidence of artificially induced calculi in your population?

Authors: It is interesting to note that your fictitious calculi incidence (1.2%) agrees with that (1%) reported by Herring (1962) and also by us in this report. However, we are not sure whether the apparent difference in incidence for foreign body nucleated calculi between Milwaukee (0.04%) and Toronto (0.3%) is actually significant as statistics from other cities are not available.

A. Rodgers: Fracture surfaces are usually selected for SEM study. Why did you use powdered specimens? Could powdering influence ultrastructure and morphology?
Authors: Wherever possible, fracture surfaces were used for SEM study. Only very small calculi were entirely powdered. Ultrastructure and morphology should be unaltered by gentle powdering.

A. Rodgers: What Mg/Ca ratios favour whitlockite deposition? Can you quote a reference?
Authors: For whitlockite to be favored in aqueous solutions resembling body fluids, Mg^{++} ions have to be present (Cheng and Pritzker, 1983) but Mg/Ca ratio should not greatly exceed 1.0 (Cheng, 1986).

A. Rodgers: What are the case histories in cases 1, 2 and 3? Were the specimens surgically removed? If so, from where? How did the plastic coated metal foil get into the patient's bladder in case 4? At surgery? How and why was the nut located in the nasal cavity (case 5)?
Authors: We regret that we are unable to answer these questions because in none of the cases were the case histories available to us.

A. Rodgers: Can you provide some literature references to nasal calculi as discussed under case 5?
Author: We are not aware of any literature references on nasal calculi and believe this report is novel.